Research Article

Xinlin Li#, Rixuan Wang#, Leilei Wang#, Aizhen Li, Xiaowu Tang, Jungwook Choi, Pengfei Zhang*, Ming Liang Jin*, and Sang Woo Joo*

Scalable fabrication of carbon materials based silicon rubber for highly stretchable e-textile sensor

https://doi.org/10.1515/ntrev-2020-0088
received September 10, 2020; accepted October 23, 2020

Abstract: Development of stretchable wearable devices requires essential materials with high level of mechanical and electrical properties as well as scalability. Recently, silicone rubber-based elastic polymers with incorporated conductive fillers (metal particles, carbon nanomaterials, etc.) have been shown to the most promising materials for enabling both high electrical performance and stretchability, but the technology to make materials in scalable fabrication is still lacking. Here, we propose a facile method for fabricating a wearable device by directly coating essential electrical material on fabrics. The optimized material is implemented by the noncovalent association of multiwalled carbon nanotube (MWCNT), carbon black (CB), and silicon rubber (SR). The e-textile sensor has the highest gauge factor (GF) up to 34.38 when subjected to 40% strain for 5,000 cycles, without any degradation. In particular, the fabric sensor is fully operational even after being immersed in water for 10 days or stirred at room temperature for 8 hours. Our study provides a general platform for incorporating other stretchable elastic materials, enabling the future development of the smart clothing manufacturing.

Keywords: e-textile sensor, carbon black, carbon nanotube, silicon rubber, mechanical properties

1 Introduction

Clothing is a necessity for human life. It provides our fellow human beings with basic functions of heatstroke prevention, cold protection, warmth, and beauty. With the continuous development of science and technology, especially of built-in e-textile sensors, the end product of clothing would be enhanced with more extended functions and better comfort. Many experts believe that smart clothing is the future development trend of the clothing industry, such as wearable sensors, monitoring human vital signs, and supercapacitors [1–5].

The uniform combination of high-performance conductive materials on fabrics is the basis for smart clothing. There have been many reports on improving mechanical properties and electronic properties of hybrid textile electronic devices based on carbon nanomaterials and silicone rubber (SR) [6,7]. Carbon material is one of the most promising materials with excellent tensile resistance and great performance in terms of hardness, heat resistance, and electrical conductivity. It has many representations, such as multiwalled carbon nanotubes (MWCNTs), carbon black (CB), graphene, and fullerene. CBs are promising electrode materials in wearable devices due to their conductive properties, electrochemical properties, and large surface

# X. L., R. W., and L. W. contributed equally to this work.

*** Corresponding author: Pengfei Zhang,** College of Electromechanical Engineering, Qingdao University, Qingdao 266071, China, e-mail: pzhang@qdu.edu.cn
*** Corresponding author: Ming Liang Jin,** Institute for Future, Qingdao University, Qingdao 266071, China; Institute for Translational Medicine, Medical College of Qingdao University, Qingdao 266071, China, e-mail: jinmingliang@qdu.edu.cn
*** Corresponding author: Sang Woo Joo,** School of Mechanical Engineering, Yeungnam University 280 Daehak-ro, Gyeongsan, Gyeongbuk 38541, Republic of Korea, e-mail: swjoo1@gmail.com, +82-53-810-2568
Xinlin Li: College of Electromechanical Engineering, Qingdao University, Qingdao 266071, China; School of Mechanical Engineering, Yeungnam University 280 Daehak-ro, Gyeongsan, Gyeongbuk 38541, Republic of Korea
Rixuan Wang, Xiaowu Tang: Department of Advanced Materials Engineering, Yeungnam University, Gyeongsan, 38541, Republic of Korea
Leilei Wang, Jungwook Choi: School of Mechanical Engineering, Yeungnam University 280 Daehak-ro, Gyeongsan, Gyeongbuk 38541, Republic of Korea
Aizhen Li: College of Textiles & Clothing, Qingdao University, Qingdao 266071, China

area [8,9]. MWCNTs play a great role in enhancing the reliability of nanomaterials due to their high strength and electrical properties [10–14]. For example, MWCNTs form bridges at Ag nanowire junctions in hybrid networks [15]. This suppresses the breakage of junctions under bending strain. With the development of MWCNTs for enhancing the potential reliability of nanomaterials, people's understanding has been increasing, and there have been many reports on the mixed structure of MWCNTs and nanomaterials [16,17]. However, few have systematically evaluated the applications of MWCNT/CB composites on fabrics [18–20].

The smart clothing is usually fabricated in two routes. The first is the bottom-up route, in which conductive materials are directly made into conductive fibers or wires used for electronic fabrics [21–25]. However, realizing large-scale e-textiles and mass production of those e-textiles by using this technique are difficult due to some technical issues, such as its potential incompatibility with the processes and equipment currently used in the textile industry [26–28]. Another way is the up-bottom route, in which the conductive material is evenly covered on the fabric by printing, or coating, to avoid the process of preparing the fabric by the bottom-up route. Nevertheless, as indicated by the most recently published work, the first route was widely used for preparing wearable electronic devices. Seldom has delved into utilizing the second route for scalable fabrication of e-textile sensors. In addition, there is a lack of research on studying the fatigue resistance of carbon material-based SR, which is significantly important if the SR composites are applied as e-textile sensors.

According to the theory of rubber elasticity, the SR composite would exhibit promising performance in wearable devices [29–31]. Therefore, in this study, a facile and large area–compatible deposition technique, namely, blade coating, was employed to produce a nanocomposite electrode on substrates. This technology has been used in many fields due to its reliability, accuracy, and film formation stability, such as organic transistors, solar cells, and electrochromic devices [32–36]. But it has to configure mixed electronic inks with different conditions at first. With a preliminary study, it is found that the increase in the MWCNT amount would improve the conductivity of MWCNT/CB/SR composites. When the ratios of CNT:CB:SR are 3/5/7/9:20:200, the resistance drops from 12.33 kΩ to 0.82 kΩ (at a measurement distance of 1 cm), but the samples with a concentration ratio of 9:20:200 were broken at 10% stretching strain due to increased cross-linking intensities [37,38]. Therefore, the concentration ratio of 7:20:200 was defined as the critical concentration. Also, the mechanical reliability of the MWCNT/CB/SR hybrid electrodes was systematically evaluated using a bending fatigue tester while imposing a large number of bending cycles (up to 5,000 times) through *in situ* resistance monitoring. By tracking the change in resistance during cyclic bending, the optimal electrode ratio was determined to obtain the best performance.

2 Experimental methods

2.1 Preparation of MWCNT/CB/SR composite electrode

The solvents used in this study were purchased from Sigma-Aldrich (ethyl alcohol (ethanol), isopropyl alcohol (IPA), acetone, and toluene). Silicone rubber (KE-441K-T) and different solvents were configured in a weight ratio and shaken for 5 h in a low-power sonic bath. MWCNT (Carbon Nanomaterial Technology, Co. Ltd) had an average diameter of 15 ± 5 nm and a length of 10 ± 2 μm. CB powder was purchased from Sigma-Aldrich (particle size of 2–12 μm, Molecular weight of 12.01). To obtain MWCNT/CB/SR composite inks, the solutions were prepared according to a mass ratio of 3:20:200, 5:20:200, 7:20:200, and 9:20:200. Then, it was stirred in one direction at 150 rpm for 5 min to obtain a uniform electronic ink colloid.

Blade coating (also known as knife coating or bar coating) is a robust process with low investment cost, suitable for rigid or flexible substrates. To deposit a thin film, an immobilized 90°-beveled razor blade (Fisher, 6 cm wide) was gently placed on a substrate (typically height is 10–500 μm). The coating solution was then placed in front of the blade that was then moved linearly across the substrate leaving a thin wet film after the blade (see Figure 1c). The razor blade offers a uniform shear force for aligning the suspended MWCNT/CB/SR composite ink. Blade coating was applied to the mask-covered fabric (Knitted Jersey, antibacterial viscose 40%, acrylic fibers 30%, model 30%) at a speed of 2 mm/s and then air dried at room temperature for 1 day to obtain a uniform electrode on the fabric.

2.2 Fatigue tests

The Bending & Stretchable Machine System (SNM, Korea) was used for stretching fatigue tests. A sourcemeter embedded with a 2634B system (KEITHLEY) was used to collect the output data. Briefly, a sample was mounted on two parallel plates. The gap between the two plates

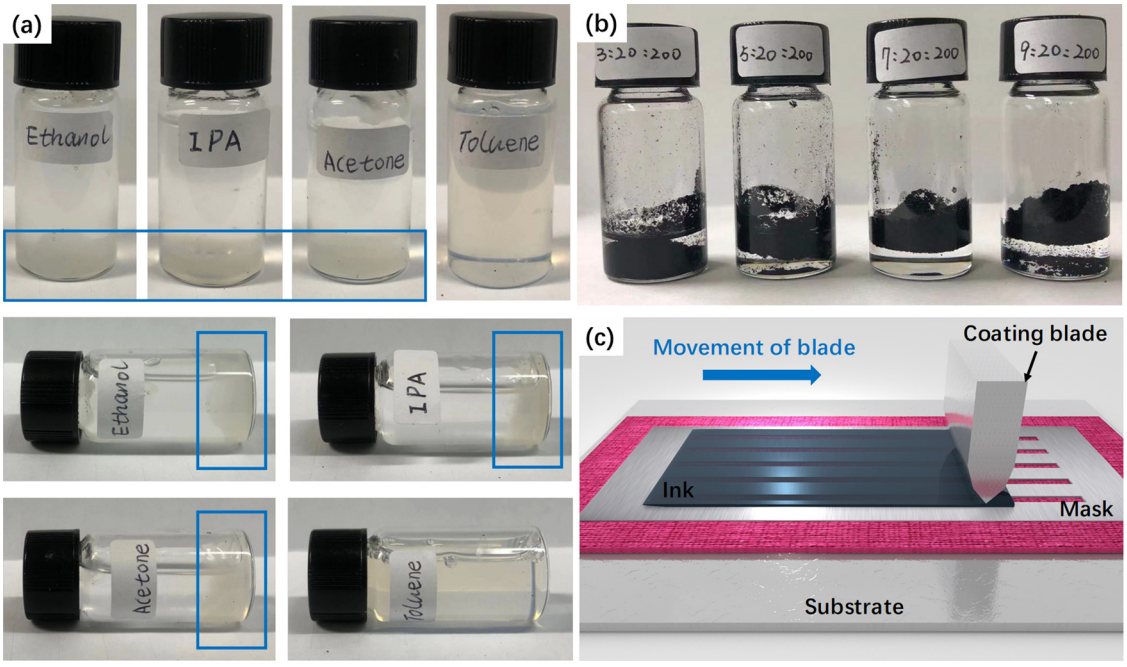

Figure 1: (a) SR diluted with ethanol, IPA, acetone, toluene to disperse (after sonication 5 h). (b) MWCNT/CB/SR composite inks formulated with a weight ratio of 3:20:200, 5:20:200, 7:20:200, and 9:20:200. (c) Blade-coating processes of MWCNT/CB/SR composites.

can be changed to adjust the nominal strain imposed on the samples. Cyclic strain experiments were performed at 0.2 Hz from 0 to 13.3% (2 mm) and then back to 0%. But stretching fatigue tests cannot simulate frequently U-type folded status of the fabric cloth. Thus, U-type folding tests at 0.2 Hz were carried out for 5,000 cycles.

2.3 Durability testing of inks

In the research that underpins this article, immersing and stirring durability of inks that were printed onto textile substrates were evaluated. We put the sample into a beaker filled with water and took it out every 2 days to air dry and measured the resistance change. We simulated the stirring experiment during washing. Here, the sample and the stirring bar were placed in a beaker and stirred at 200 rpm for 8 h, and the resistance change was measured after air drying every 2 hours.

2.4 Characterization of morphology and conductivity

The morphologies of the MWCNT/CB/SR conductive lines were investigated using optical microscopy (OM; Nikon ECLIPSE LV100ND) and scanning electron microscopy (SEM; Hitachi S4800). Electrical conductivities of the MWCNT/CB/SR composite material wires were measured with a two-probe method using a TK-3200A digital multimeter (TAE KWANG ELECTRONICS CO. Korea). The diameter of the probe is 2 mm. The pierce depth was controlled at 100 μm.

3 Results and discussions

3.1 Mixing strategy for inks

Studies have shown that too high ink surface tension is not conducive for blade coating [39]. Therefore, we first diluted the SR using ethanol, IPA, acetone, and toluene respectively and disperse them in sonication for 5 h. It was found that, only in toluene, it can be dispersed uniformly. The remaining composited solution has obvious precipitation at the bottom (see Figure 1a). Other solutions were also prepared according to the mass ratios of SR to toluene at 1:5, 1:3, and 1:1. To make a solution suitable for direct coating, the concentration has to be decently low. The effect of solution concentration on the mechanical property of SR was investigated by running tensile tests on SR sample. Figure 2 shows the stress–strain curves for SR samples after the tensile tests.

Obviously the SR sample mixing without any toluene owns highest stress and toughness. For SR samples mixing with toluene, the ratio at 1:1 enables the sample owns highest strain at break, as high as 268.70%. If applied to the e-textile application, the strain at break is the priority that needs be considered seriously for sensors. Thus, the best mixing ratio of SR to toluene is determined as 1:1.

(a)

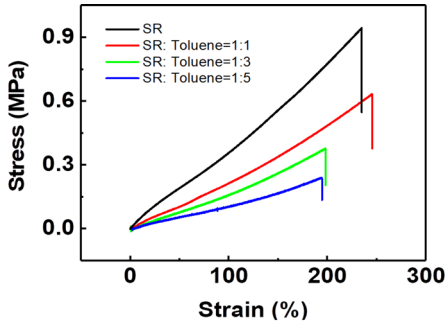

(b)

	SR	1:1	1:3	1:5
Stress (MPa)	0.94	0.82	0.50	0.32
Strain (%)	246.82	268.70	203.72	198.65
Surface tension (mN/m)	28.25	23.79	24.83	25.20

Figure 2: (a) The relationship between strain (%) and stress (MPa) formulated with pure SR and weight ratio of SR to toluene, 1:1, 1:3, 1:5 (after sonication 5 h). (b) The stress, strain, and surface tension for the various weight ratios of SR/toluene solutions.

3.2 Coated electrodes

The other studies have shown that the tensile and tear strength of the rubber composites containing MWCNTs were lower than those of the rubber filled with CB, which might be due to MWCNTs agglomerates in rubber matrix [40]. So here CBs was chosen as the main conductive material and MWCNT was selected as the reinforcing agent, acting as "bridges" among CB/SR, similar to the work in which MWCNTs forms bridges at Ag nanowire junctions in hybrid networks [15]. In our previous study, it was shown that the uniform dispersion of MWCNT and CB is a very complicated process when preparing inks [41,42]. Here, we made MWCNT/CB/SR into conductive inks through a facile stirring process. To study the effect of the concentration of MWCNT on electrical properties, it is guarantee that MWCNT with different amounts were added under the same conditions of CB (fixed at 20 g) and SR (fixed at 200 g). The amount of MWCNT was set at 3, 5, 7, and 9 g. Figure 1b shows the MWCNT/CB/SR composite inks formulated with ratios at 3:20:200, 5:20:200, 7:20:200, and 9:20:200. After stirring for 5 min, a uniform composite conductive ink was obtained, and conductive wires were prepared on the fabric at a speed of 2 mm/s and a height of 50 μm by means of blade coating (see Figure 3a). The relationship between the measurement distance and the electrical resistance is shown in Figure 3b. The change of electrical resistance is remarkable when comparing the 5:20:200 sample with 3:20:200 sample. But the electrical resistance barely changes for 7:20:200 and

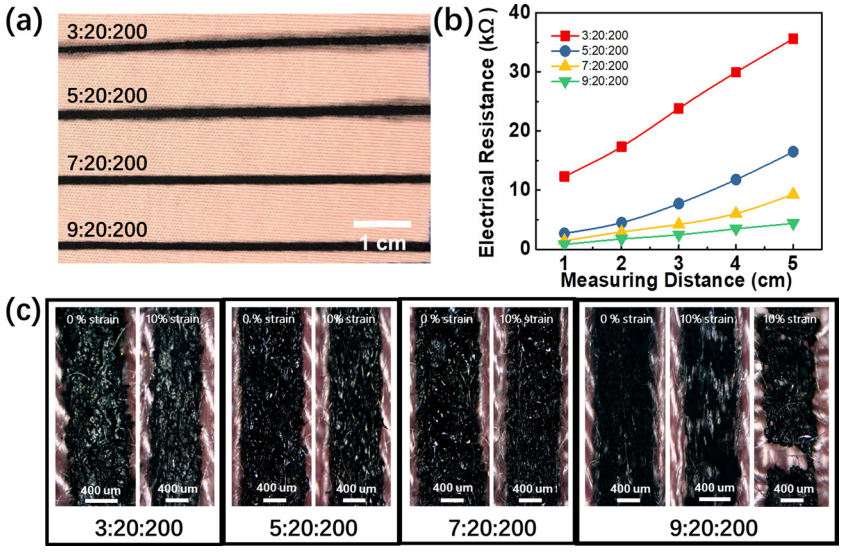

Figure 3: (a) Blade coating on fabric for different MWCNT/CB/SR composite electrodes. (b) Relationship of electrical resistance and measuring distance. (c) Virgin and 10% stretched electrodes.

9:20:200 samples. It has been pointed out that very low percolation thresholds exist for MWCNT composites [43]. Therefore, adding more MWCNT leads to a decrease in the resistance by at least a factor.

3.3 Morphology of electrode surface

SEM images of the MWCNT/CB/SR composite electrode were used to analyze morphological changes of the electrode surface, as shown in Figure 4. These images do not reveal if there is a gel-like zone at low magnification, such as ×100, ×500, and ×1,000. But it is clear to see gel-like zones at the magnification ×10,000 for samples with ratios at 3:20:200 and 5:20:200. By using a software tool Nano Measurer, the area of gel-like zone takes about 63% for 3:20:200 sample; and it reduces to about 30% for 5:20:200 sample. It is hardly to see gel-like zone for samples with ratios at 7:20:200 and 9:20:200. This is why the resistance of the guide electrode is reduced. Moreover, as shown in Figure 3a, coated electrode spreads out on the textile when solutions with ratios are at 3:20:200 and 5:20:200. Such an issue can easily cause electrical shortage under voltage supplies. The spreading-out problem disappears when they are at 7:20:200 and 9:20:200. It seems the printed conductive wires with higher MWCNT content have better printing quality. In comparison to less MWCNT content, it is hard to see penetration marks for wires with ratios at 7:20:200 and 9:20:200. However, the wires with ratio at 9:20:200 were broken when stretched to a 10% strain, as shown in Figure 3c. When compared, the other wires exhibited excellent stretchability. The excellent stretchable performance might be due to increased cross-linking intensities within molecular network [37,38].

3.4 Evaluation of performance as wearable devices

The adhesion of the coated electrode on the surface of the fabric was characterized by peeling electrode layer off a substrate with transparent tape (see Figure 5a). Then, it was completely immersed in water and then removed from the water after 0, 2, 4, 6, 8, and 10 days, respectively. As shown in Figure 5b, the resistance remains the same except for the sample with ratio at 3:20:200, which fluctuates slightly. Also after stirring the sample at 200 rpm for 8 h, no obvious change in resistance was found (Figure S1 in supplementary information). It proves that the electronic inks have remarkable stability. An LED lamp was pasted between two conductive wires near the coating, which were wrapped around a glass beaker with a diameter of 2 and 1.5 cm. Then, an external electrical power was applied to the LED lamp. As shown in Figure 5c, the LED lamp still functionally works. U-type folding tests at

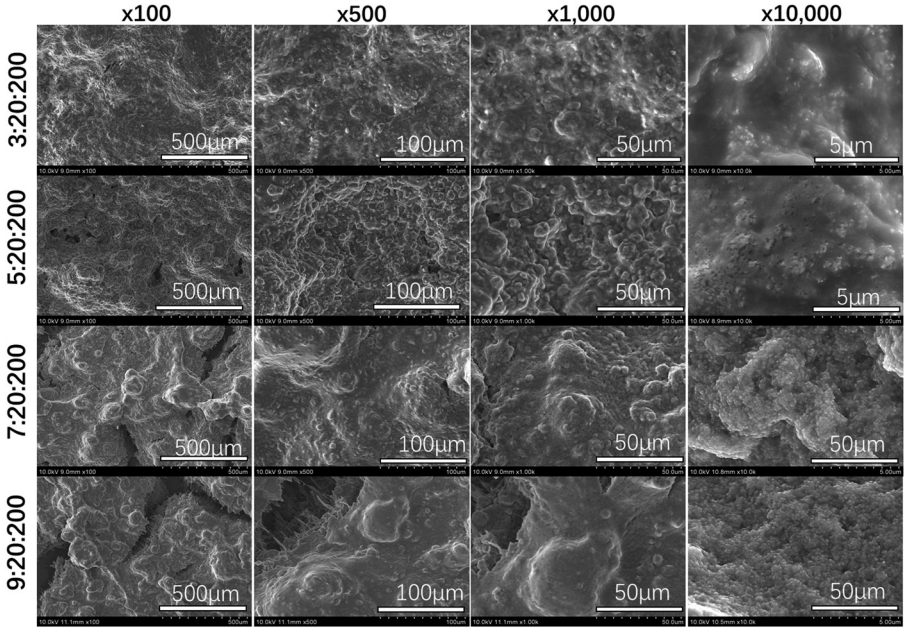

Figure 4: SEM images of the blade coated MWCNT/CB/SR electrodes under different magnification from ×100 to ×10,000.

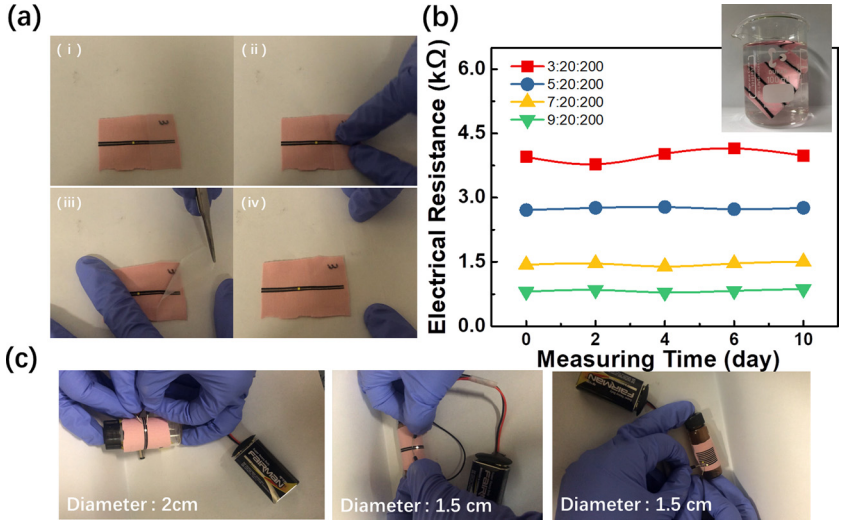

Figure 5: (a) Peeling off the electrodes layer with scotch tape. (b) The relationship of electrical resistance and measuring days (completely immersed in water). (c) Conductivity measurement under different bending conditions.

0.2 Hz for 5,000 cycles also prove that the electrode exhibits promising stability and stretchability (shown in Figure S2 in supplementary information). Of course, not only on the fabric, the U-type folding tests were also conducted on many other substrates. It was found that the same coating conditions show a uniform pattern on various substrates, such as 3 M tape, paper, and poly(ethylene terephthalate) (PET) film (Figure S3b in supplementary information).

Figure 6 shows the standardized resistance change of the sensor under various strain values. The performance of a strain sensor could be evaluated by a gauge factor (GF). The working voltage of the sensor was set at 1 V. The relative change of the resistance (RCR, %) is calculated based on the resistance measured by using equation (1):

$$\frac{\Delta R}{R_0} = \frac{(R_s - R_0)}{R_0} \times 100\% \tag{1}$$

where ΔR is the change of resistance and R_0 and R_s are the resistance without and with applied strain, respectively. Furthermore, the GF of the strain sensor, defined as in equation (2) [39,40]:

$$\mathrm{GF} = \frac{(\Delta R/R_0)}{\epsilon} \tag{2}$$

where ϵ denotes the applied strain, which is calculated according to $\epsilon = 100 \times \Delta L/L_0$ based on the RCR–strain curves, where ΔL is the change of length and L_0 is the original length.

Figure 6a and e show the I–V curve of the 5:20:200 and 7:20:200 sensors at different stretching length, respectively. From both I–V curves, it clearly shows that electrical resistance increases along with the increase in the stretching length. Regardless of the applied strain, the sensor exhibits ohmic characteristics [23,44], and the current decreases monotonically with the increasing tensile strain. It seems that the initial resistance of the device can be controlled by changing the proportion of MWCNT. According to the RCR–strain curves in Figure 6b and f, the sample GF with ratio at 5:20:200 was calculated as 24.89 (0–20% stretch range), while it became as 10 (0–20% stretch range) and 34.38 (20–40% stretch range) for the sample with ratio at 7:20:200. It is worth noting that the applied strain limits are 20% and 40% for samples at 5:20:20 and 7:20:200, respectively. Under the same strain 20%, for example, the 7:20:200 sample has lower GF than the 5:20:200 sample. This is because the interlaced MWCNTs and CBs increased with the increase of MWCNT amount. Under the same stretch, the samples with higher MWCNTs amount have more conductive paths, and thus, the resistance change is smaller. Within the 20% stretch range, the 7:20:200 sample has a lower gauge factor. But the stretching range of the 7:20:200 sample is larger than that of the 5:20:200 sample. As shown in Figure 6c and g, the sensor has undergone a cyclic strain test at 0.2 Hz in the range of 0–13.3% (2 mm)–0%. The sample maintains stable performance over 5,000 cycles. The decrease in $\Delta R/R_0$ at the beginning of the experiment can be explained by the accumulative relaxation of the MWCNT/CB, leading to a decrease in device sensitivity [45–47]. Figure 6d and e show the first single stretch-recovery cycle of the device (MWCNT/CB/SR weight ratio at 5:20:200 and 7:20:200, respectively). The peak that appears during the recovery process can be explained by the recombination and restacking of the nanomaterials [48].

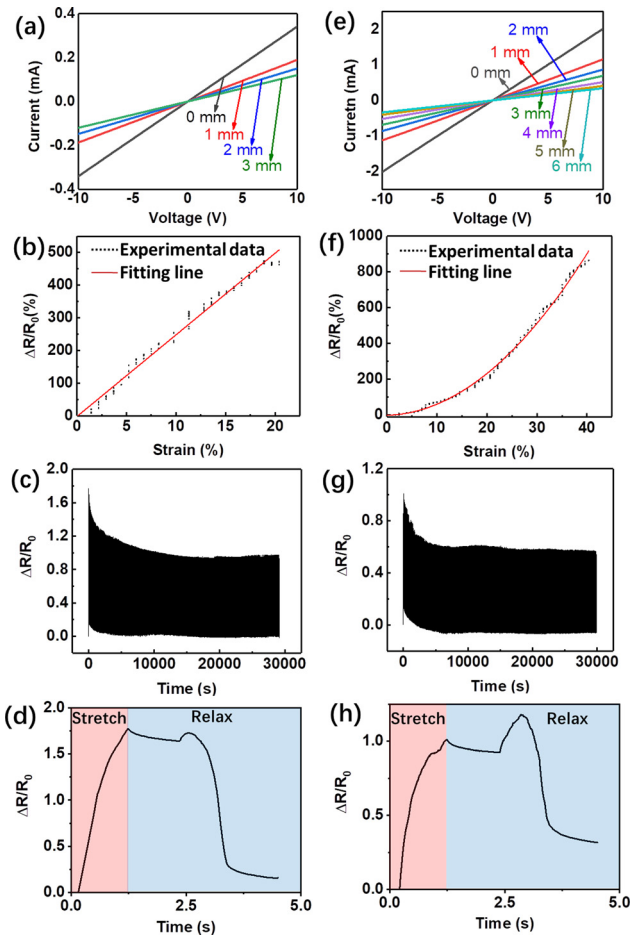

Figure 6: (a) Linear *I–V* curve of the 5:20:200 sample at different stretching length. (b) Resistance changes of the 5:20:200 sample with respect to the applied tensile strain from 0 to 20%. (c) Resistance changes of the 5:20:200 sample under cyclic tensile strain from 0 to 5% for 5,000 cycles. (d) Illustration of a single cycle of 5:20:200 sample. (e) Linear *I–V* curve of the 7:20:200 sample at different stretching length. (f) Resistance changes of the 5:20:200 sample with respect to the applied tensile strain from 0 to 40%. (g) Resistance changes of the 7:20:200 sample under cyclic tensile strain from 0 to 50% for 5,000 cycles. (h) Illustration of a single cycle of 7:20:200 sample.

For the transient delay of $\Delta R/R_0$ at the initial stage of recovery process, it speculates that it is caused by the fixing effect of silica gel on the nanomaterials.

4 Conclusion

In summary, the effect of adding MWCNTs on the electrical and mechanical properties of wearable devices was investigated for MWCNT/CB/SR composite electrodes. The electrical property of the composite material was enhanced along with an increase in the MWCNT concentration. By evaluating the printing quality and mechanical performance, the critical concentration ratio of MWCNT/CB/SR was optimized at 7:20:200. The resistance remained the same with slight fluctuation after the sample was immersed in water for 10 days and stirred at 200 rpm for 8 h, indicating that the sample has remarkable waterproof performance. Bending fatigue tests were performed under the condition of 5:20:200 and 7:20:200. The results revealed that the mechanical reliability increased remarkably of MWCNT/CB/SR composites electrode at 7:20:200. When the stretch strain range reaches at 0–20% and 20–40%, the gauge factor (GF) was calculated as 10 and 34.38, respectively. The 5,000-cycle bending fatigue test also showed that the e-textile sensor owns excellent stability. Based on these results, we concluded that MWCNT/CB/SR hybrid electrode with ratio at 7:20:200 is the optimal concentration for the best performance and as the application of hybrid electrodes to flexible electronics.

Acknowledgements: The authors gratefully acknowledge support from the Grant NRF-2018R1A2B3001246, Science and Technology Support Plan for Youth Innovation of Colleges in Shandong Province (DC2000000891), and the Young Taishan Scholars Program of Shandong Province (No. 201909099).

Conflict of interest: The authors declare no conflict of interest regarding the publication of this paper.

References

[1] Bariya M, Nyein HYY, Javey A. Wearable sweat sensors. Nat Electron. 2018;1(3):160.
[2] Khan Y, Ostfeld AE, Lochner CM, Pierre A, Arias AC. Monitoring of vital signs with flexible and wearable medical devices. Adv Mater. 2016;28(22):4373–95.
[3] Majumder S, Mondal T, Deen MJ. Wearable sensors for remote health monitoring. Sensors. 2017;17(1):130.
[4] Choi C, Lee JM, Kim SH, Kim SJ, Di J, Baughman RH. Twistable and stretchable sandwich structured fiber for wearable sensors and supercapacitors. Nano Lett. 2016;16(12):7677–84.
[5] Du D, Li P, Ouyang J. Graphene coated nonwoven fabrics as wearable sensors. J Mater Chem C. 2016;4(15):3224–30.
[6] Guo X, Huang Y, Cai X, Liu C, Liu P. Capacitive wearable tactile sensor based on smart textile substrate with carbon black/silicone rubber composite dielectric. Meas Sci Technol. 2016;27(4):045105.

[7] Mun TJ, Kim SH, Park JW, Moon JH, Jang Y, Huynh C, et al. Wearable energy generating and storing textile based on carbon nanotube yarns. Adv Funct Mater. 2020;30(23):2000411.
[8] Gao M, Zheng F, Xu J, Zhang S, Bhosale SS, Gu J, et al. Surface modification of nano-sized carbon black for reinforcement of rubber. Nanotechnol Rev. 2019;8(1):405–14.
[9] Pan U, Xu K, Wu C. Recent progress in supercapacitors based on the advanced carbon electrodes. Nanotechnol Rev. 2019;8(1):299–314.
[10] Lu H, Min Huang W. Synergistic effect of self-assembled carboxylic acid-functionalized carbon nanotubes and carbon fiber for improved electro-activated polymeric shape-memory nanocomposite. Appl Phys Lett. 2013;102(23):231910.
[11] Lu H, Liang F, Gou J. Nanopaper enabled shape-memory nanocomposite with vertically aligned nickel nanostrand: controlled synthesis and electrical actuation. Soft Matter. 2011;7(16):7416–23.
[12] Nah C, Lim JY, Cho BH, Hong CK, Gent AN. Reinforcing rubber with carbon nanotubes. J Appl Polym Sci. 2010;118(3):1574–81.
[13] Li Z, Xu K, Pan Y. Recent development of supercapacitor electrode based on carbon materials. Nanotechnol Rev. 2019;8:35–49.
[14] Power AC, Gorey B, Chandra S, Chapman J. Carbon nanomaterials and their application to electrochemical sensors: a review. Nanotechnol Rev. 2018;7(1):19–41.
[15] Hwang B, Li X, Kim SH, Lim S. Effect of carbon nanotube addition on mechanical reliability of Ag nanowire network. Mater Lett. 2017;198:202–5.
[16] Nam I, Park SM, Lee H-K, Zheng L. Mechanical properties and piezoresistive sensing capabilities of FRP composites incorporating CNT fibers. Composite Struct. 2017;178:1–8.
[17] Lee J, Morita M, Takemura K, Park EY. A multi-functional gold/iron-oxide nanoparticle-CNT hybrid nanomaterial as virus DNA sensing platform. Biosens Bioelectron. 2018;102:425–31.
[18] Singh PSS, Condon K, Sachinvala B, Hui N, Scope D. of nanotechnology in modem textiles. World J Eng. 2010;7(1):1–4.
[19] Li Z, Xu K, Pan Y. Recent development of supercapacitor electrode based on carbon materials. Nanotechnol Rev. 2019;8(1):35–49.
[20] Ossai CI, Raghavan N. Nanostructure and nanomaterial characterization, growth mechanisms, and applications. Nanotechnol Rev. 2018;7(2):209–31.
[21] Pahalagedara LR, Siriwardane IW, Tissera ND, Wijesena RN, de Silva KN. Carbon black functionalized stretchable conductive fabrics for wearable heating applications. RSC Adv. 2017;7(31):19174–80.
[22] Lai YC, Deng J, Zhang SL, Niu S, Guo H, Wang ZL. Single-thread-based wearable and highly stretchable triboelectric nanogenerators and their applications in cloth-based self-powered human-interactive and biomedical sensing. Adv Funct Mater. 2017;27(1):1604462.
[23] Li Y-Q, Huang P, Zhu W-B, Fu S-Y, Hu N, Liao K. Flexible wire-shaped strain sensor from cotton thread for human health and motion detection. Sci Rep. 2017;7:45013.
[24] Sawhney P, Allen H, Reynolds M, Slopek R, Condon B, Hui D, et al. Effect of web formation on properties of hydroentangled nonwoven fabrics. World J Eng. 2012;9:407–16.
[25] Sawhney APS, Condon B, Singh KV, Pang S-S, Li G, Hui D. Modern applications of nanotechnology in textiles. Text Res J. 2008;78(8):731–9.
[26] Wu C, Kim TW, Li F, Guo T. Wearable electricity generators fabricated utilizing transparent electronic textiles based on polyester/Ag nanowires/graphene core–shell nanocomposites. ACS Nano. 2016;10(7):6449–57.
[27] Jost K, Stenger D, Perez CR, McDonough JK, Lian K, Gogotsi Y, et al. Knitted and screen printed carbon-fiber supercapacitors for applications in wearable electronics. Energy Environ Sci. 2013;6(9):2698–705.
[28] Sawhney P, Reynolds M, Allen C, Condon B, Slopek R, Hinchliffe D, et al. Greige cotton comber noils for sustainable nonwovens. World J Eng. 2011;8:291–4.
[29] Lu H, Liu Y, Leng J, Du S. Qualitative separation of the physical swelling effect on the recovery behavior of shape memory polymer. Eur Polym J. 2010;46(9):1908–14.
[30] Lu H, Du S. A phenomenological thermodynamic model for the chemo-responsive shape memory effect in polymers based on Flory–Huggins solution theory. Polym Chem. 2014;5(4):1155–62.
[31] Lu H, Leng J, Du S. A phenomenological approach for the chemo-responsive shape memory effect in amorphous polymers. Soft Matter. 2013;9(14):3851–8.
[32] Kim YA, Hayashi T, Endo M, Gotoh Y, Wada N, Seiyama J. Fabrication of aligned carbon nanotube-filled rubber composite. Scr Materialia. 2006;54(1):31–5.
[33] Kim TA, Kim HS, Lee SS, Park M. Single-walled carbon nanotube/silicone rubber composites for compliant electrodes. Carbon. 2012;50(2):444–9.
[34] Kondo M, Kajitani T, Uemura T, Noda Y, Ishiwari F, Shoji Y, et al. Highly-ordered triptycene modifier layer based on blade coating for ultraflexible organic transistors. Sci Rep. 2019;9(1):9200.
[35] Kim K, Hong J, Hahm SG, Rho Y, An TK, Kim SH, et al. Facile and microcontrolled blade coating of organic semiconductor blends for uniaxial crystal alignment and reliable flexible organic field-effect transistors. ACS Appl Mater Interfaces. 2019;11(14):13481–90.
[36] Razza S, Di Giacomo F, Matteocci F, Cina L, Palma AL, Casaluci S, et al. Perovskite solar cells and large area modules (100 cm^2) based on an air flow-assisted PbI_2 blade coating deposition process. J Power Sources. 2015;277:286–91.
[37] Zhao W, Zhang S, Zhang Y, Li S, Liu X, He C, et al. Environmentally friendly solvent-processed organic solar cells that are highly efficient and adaptable for the blade-coating method. Adv Mater. 2018;30(4):1704837.
[38] Howard IA, Abzieher T, Hossain IM, Eggers H, Schackmar F, Ternes S, et al. Coated and printed perovskites for photovoltaic applications. Adv Mater. 2019;1806702.
[39] Yang Z, Chueh CC, Zuo F, Kim JH, Liang PW, Jen AKY. High-performance fully printable perovskite solar cells via blade-coating technique under the ambient condition. Adv Energy Mater. 2015;5(13):1500328.
[40] Hamed GR. Reinforcement of rubber. Rubber Chem Technol. 2000;73(3):524–33.
[41] Li X, Jeong YJ, Jang J, Lim S, Kim SH. The effect of surfactants on electrohydrodynamic jet printing and the performance of organic field-effect transistors. Phys Chem Chem Phys. 2018;20(2):1210–20.

[42] Li X, Go M, Lim S, An TK, Jeong YJ, Kim SH. Electrohydrodynamic (EHD) jet printing of carbon-black composites for solution-processed organic field-effect transistors. Org Electron. 2019;73:279–85.
[43] Gao L, Zhou X, Ding Y. Effective thermal and electrical conductivity of carbon nanotube composites. Chem Phys Lett. 2007;434(4):297–00.
[44] Park H, Kim DS, Hong SY, Kim C, Yun JY, Oh SY, et al. A skin-integrated transparent and stretchable strain sensor with interactive color-changing electrochromic displays. Nanoscale. 2017;9(22):7631–40.
[45] Lin L, Liu S, Zhang Q, Li X, Ji M, Deng H, et al. Towards tunable sensitivity of electrical property to strain for conductive polymer composites based on thermoplastic elastomer. ACS Appl Mater interfaces. 2013;5(12):5815–24.
[46] Chen L, Chen G, Lu L. Piezoresistive behavior study on finger-sensing silicone rubber/graphite nanosheet nanocomposites. Adv Funct Mater. 2007;17(6):898–904.
[47] Gao L, Thostenson ET, Zhang Z, Chou TW. Sensing of damage mechanisms in fiber-reinforced composites under cyclic loading using carbon nanotubes. Adv Funct Mater. 2009;19(1):123–30.
[48] Pan F, Chen SM, Li Y, Tao Z, Ye J, Ni K, et al. 3D graphene films enable simultaneously high sensitivity and large stretchability for strain sensors. Adv Funct Mater. 2018;28(40): 1803221.